European Journal of Applied Sciences – Vol. 13, No. 01
Publication Date: February 25, 2025
DOI:10.14738/aivp.1301.18366.
Murayama, R. (2025). Examination of Pole Structure for Static Magnetic Field Constituting Electromagnetic Acoustic Transducer (EMAT) for Lamb Wave Using Electromagnetic Induction Coil with Ferromagnetic Core. European Journal of Applied Sciences, Vol - 13(01). 453-464.

Examination of Pole Structure for Static Magnetic Field Constituting Electromagnetic Acoustic Transducer (EMAT) for Lamb Wave Using Electromagnetic Induction Coil with Ferromagnetic Core

Riichi Murayama
Fukuoka Institute of Technology, Japan;
3-30-1 Wazirohigashi, Higashi, Fukuoka, 811-0295, Japan

ABSTRACT
To increase the mechanical and thermal strengths of the EMAT for Lamb waves, the air-core electromagnetic induction coil that constitutes the EMAT was changed to a structure in which a conductor is wound around a ferromagnetic material. Initially, the coils for the static and dynamic magnetic fields were vertically wound around low-carbon steel, a ferromagnetic material. As a result, a transmission signal was detected. To further improve the received signal strength, a structure separating the poles for the static and dynamic magnetic fields was evaluated. It was then confirmed that an improvement in the received signal strength was obtained. Conventionally, the magnetic poles for a static magnetic field and dynamic magnetic field were alternately arranged. In the present paper, the structure was changed to a two-pole structure for the static magnetic poles, and all the dynamic magnetic poles were sandwiched between the two poles. As a result, a dramatic improvement in the sensitivity was achieved.

Keywords: Lamb wave, EMAT, Nondestructive inspection, EM-coil, Ferromagnetic core.

INTRODUCTION
Ultrasonic waves are widely used as the most effective means in the nondestructive testing of materials and structures. Lamb waves, a type of ultrasonic waves, are used as an effective means for the large-scale inspection of cold-rolled steel plates, hot-rolled steel plates, steel pipes, etc. [1-3]. An ultrasonic sensor for the Lamb wave used for the on-line inspection of cold-rolled and hot-rolled steel sheets is tire-shaped in appearance. This ultrasonic probe enables the on-line full-length inspection by rotating the tire-shaped case in the rolling direction. Longitudinal ultrasonic waves transmitted from a piezoelectric transducer mounted inside the tire are transmitted at an angle to the steel plate, and Lamb waves are transmitted and received inside the steel plate by mode conversion. It is also necessary to continuously apply oil or other contact mediums to the contact points of the steel plate surface with the tire-shaped probe. However, unevenness in the coating of the contact medium occurs, and the detection sensitivity fluctuates dramatically [4]. In recent years, various kinds of inspections of pipes and outer walls of structures have been investigated by taking advantage of the characteristics of the Lamb waves. For example, it is known that the temperature of heat exchangers used in power plants rises to about 500°C [5-8]. However, general piezoelectric transducer ultrasonic probes are designed to be used at room temperature and cannot be used at temperatures above 50°C for

long periods of time. Electromagnetic acoustic transducers (EMATs) were originally proposed as ultrasonic transducers that do not require a contact medium and can be applied to structures and materials that are essentially hot. However, several issues became apparent during the development process. One of the problems is that the separation distance between the EMAT and the specimen surface is extremely small, only a few millimeters. As a result, thermal damage when applied to hot objects and mechanical damage due to collisions when applied to moving objects became major problems. In other words, the electromagnetic induction coil that constitutes the EMAT is structurally vulnerable to thermal and mechanical damages, which prevents the EMAT from being applied to moving objects and high-temperature structures [9-10]. There are some cases of EAMTs that were specifically developed for use in high-temperature structures [11], but they require cooling facilities and are not easy-to-use ultrasonic sensors.

The purpose of this study is to develop an EMAT that is resistant to thermal and mechanical damages by changing the structure of the electromagnetic induction coil to one in which the conductors are wound around a ferromagnetic core [12]. The resulting improved EMAT should be measurable while in contact with hot objects. First, we decided to examine a Lamb wave EMAT for thin plate inspection. As a first step, we examined a type of EMAT that is based on the principle that bias magnetic field generation is also simultaneously performed using magnetic poles for AC magnetic field generation [13]. The results of the evaluation test showed that EMAT was noticeably less sensitive in this structure. Therefore, a structure was made to separate the magnetic poles for DC and AC magnetization; the magnetic pole for the AC magnetization was made of the PC Perm-alloy. As a result, the sensitivity was dramatically improved [14]. However, the magnetic permeability of the Perm-alloy rapidly drops at temperatures above 100°C, making it difficult to apply it to high-temperature structures, which is one of the features of the EMAT. Therefore, in this paper, we reexamined the structure of the magnetic pole material as a steel whose properties can be maintained up to nearly 800°C. The results are now reported.

BASIC STRUCTURE OF CONVENTIONAL EMAT FOR LAMB WAVES [9,10]

Figure 1 shows the vibration pattern of a Lamb wave, which propagates along the thin plate surface in the right direction on the paper surface, while the vibration pattern oscillates in the vertical direction on the front and the horizontal direction of the thin plate at regular intervals.

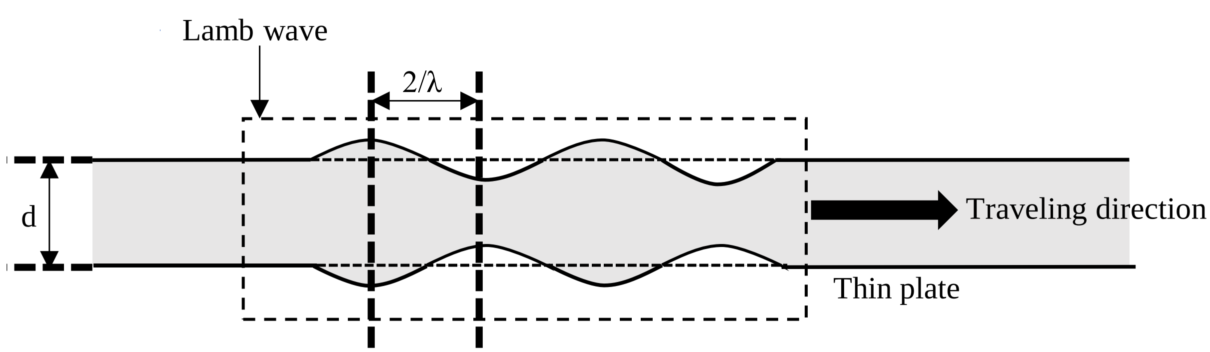

Fig.1: Vibration pattern of Lamb wave

The ratio of the vertical to horizontal components of the Lamb wave calculate using equation (1). Using the values described in the later section on experimental conditions, a plate thickness of 0.8 mm and a drive frequency of 200 kHz, the result is approximately 0.12. The horizontal displacement component is overwhelmingly dominant. This means that the Lamb wave EMAT under these conditions should provide vibration displacement in the horizontal traveling direction.

$$\frac{\eta}{\xi} = \frac{P^2-1}{2P} \cdot \tan(kpd) \quad (1)$$

η: Vertical vibration component, ***ξ***: Horizontal vibration component
k: Wavenumber (**2π/λ**), d: Plate thickness, V_t: Velocity of transverse wave, V_p: Phase velocity of Lamb wave
P= $((V_p/ V_t)^2-1)_{1/2}$

Two types of EMATs for Lamb waves exist: the first type uses the Lorentz force, which is the most well-known source of driving EMATs. The other type uses the magnetostrictive effect. The former is applicable to any metallic material, while the latter is applicable only to ferromagnetic materials that can generate magnetostriction. Figure 2(a) shows a type that uses Lorentz force and consists of a comb-shaped electromagnetic induction coil that reverses the direction of the current at regular intervals and a magnet that provides a magnetic field in the vertical direction of the thin specimen. The Lorentz force is generated in the vertical direction of the electrodes of the comb-shaped induction coils by the interaction between the induced current and the static magnetic field generated on the surface of the metal specimen directly under the comb-shaped induction coils. Since the direction of the current flowing between adjacent comb-shaped electromagnetic induction coil electrodes is reversed, the direction of the Lorentz force is also 180 degrees in the opposite direction. If the distance between these electrodes matches half of the Lamb wave wavelength to be generated, then the Lamb wave is the driving source. Figure 2(b) shows a type that uses the magnetostrictive effect. Magnets are placed on both sides of the comb electromagnetic induction coil to achieve a horizontal magnetic field on the comb electromagnetic induction coil. In this case, an induced magnetic field is generated on the surface of the metal material in a direction parallel to the metal surface and perpendicular to the electrodes due to the current flowing through the electrodes of the comb-type electromagnetic induction coil. Magnetostriction is generated in the direction parallel to this induced magnetic field. The direction of the magnetostriction between adjacent electrodes is reversed 180 degrees, and when the distance between these adjacent magnetostrictions is half the Lamb wave wavelength, the Lamb wave is generated. In the case of the magnetostriction effect type (Figure 1(b)), Lorentz force in the vertical direction is generated in principle, but it is considered to be smaller than the magnetostriction effect. The reason is that in the case of ordinary steel, when a static magnetic field of about 100mT, which is the most likely to generate magnetostriction, is applied, the magnitude of magnetostriction due to the dynamic magnetic field is expected to be about 5nm. In contrast, the Lorentz force is the product of the magnetic flux density, current, and electrode length, as in equation (2). Assuming that the length of the electrode is 10 mm used in this experiment and that the magnitude of 1(A) directly energizing the comb-type electromagnetic induction coil flows directly to the opposing metal surface, the calculated Lorentz force is about 0.001(N). If the longitudinal modulus of elasticity of ordinary steel is approximately 20 kgf/m^3, the magnitude of strain due to Lorentz force is considered to be about 0.5 (nm) based on equation (3). In this experiment, we proceeded with a study based on the magnetostrictive effect type, in which the required static magnetic field is 100 mT, which can be sufficiently realized even with a permanent magnet.

The receiving principle is to detect the induced current generated by the electromagnetic induction phenomenon that occurs in the presence of an ultrasonic vibration and a magnetic field. The actual structure of the EMAT is the same as that for transmission. The induction phenomenon is proportional to the magnitude of the magnetic permeability of the steel plate. The way the magnetic permeability changes also depend on the magnitude of the magnetic field given to the thin plate, and there is an optimum value. The correlation is not the same as the relationship between the magnetostriction and bias magnetic field, but it is quite similar, and optimal values exist in the range of 50mT to 100mT. In the case of this structure, there were issues of damage due to contact with the test material and thermal damage in the case of high-temperature materials.

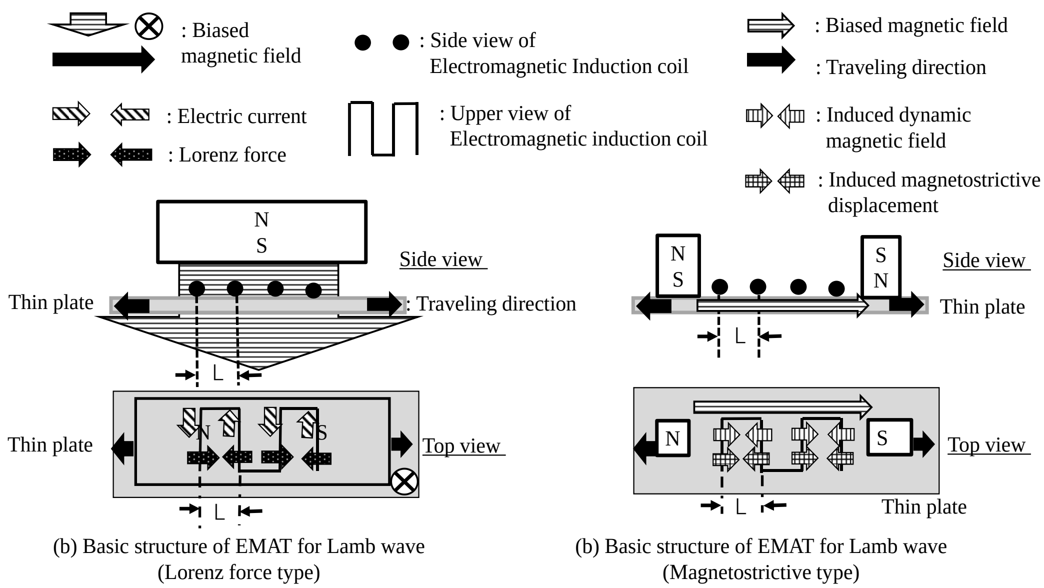

Fig.2: Basic structure of a conventional EMAT for Lamb wave

Figure 3 shows the ultrasonic velocity of the generated Lamb wave in relation to the driving frequency, where S_0 mode and A_0 mode exist in the frequency range below 1MHz. We attempted to try to detect the S_0 mode Lamb wave of the 200 kHz driving frequency in this study. In this case, the wavelength is about 10 mm using equation (2), and the electrode spacing (L) is 5 mm.

$$V(m/s) = \lambda(m) \times f(1/s) \quad (2)$$

λ: Wave length, f: Frequency

$$Velocity = \lambda(wave\ length) \times f(frequency)$$

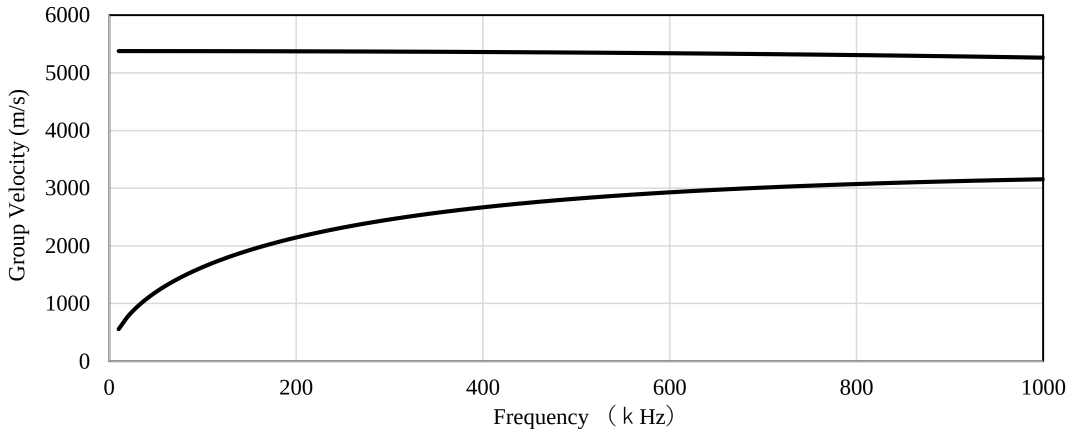

Fig.3: Relationship between driving frequency and group velocity of Lamb wave

ELECTROMAGNETIC INDUCTION COIL WITH FERROMAGNETIC POLES

Figure 4 shows a conceptual diagram for solving the problem of the EMAT for ordinary Lamb waves. Figure 4(a) is a diagram and a photograph of the electromagnetic induction coil section picked up from Figures 2(a) and 2(b). Figure 4(b) shows magnetic poles with conductors wrapped around them instead of the regularly spaced electrodes in Figure 4(a). As a result, we considered that the area in close proximity to the material surface would be drastically reduced from being damaged by heat or mechanical shock. Figure 5 shows a photograph of an EMAT for Lamb waves using an electromagnetic induction coil with ferromagnetic poles. Figure 5(a) shows a coil for static magnetic field generation wound on top of an electromagnetic induction coil with ferromagnetic poles. Although the received signal was confirmed for this structure, its signal strength was extremely low. In Figure 5(b), the magnetic poles for the dynamic magnetic field are separated and placed between the magnetic poles for the static magnetic field to overcome this problem. As a result, the received signal strength was improved. However, the received signal strength was not enough, so we changed to a structure in which the magnetic poles for the static magnetic field are placed between all the magnetic poles for the dynamic magnetic field, as shown in Figure 5(c). In this paper, the improvement of Fig. 5(c) is described. In both cases, the spacing between the poles for the dynamic magnetic field is adjusted to half the Lamb wave wavelength to be generated. In this case, the driving frequency was 200 kHz, so the distance was 5 mm. Figure 6 shows a drawing of the structures shown in Figures 5(b) and 5(c). The horizontal magnetic flux density directly below the dynamic magnetic field poles is measured by a Gauss meter. When the dynamic and static magnetic field poles are arranged alternately (Type A), the magnetic flux density values under all the dynamic magnetic field poles are almost the same, but when all dynamic magnetic field poles are sandwiched together (Type B), the value under the dynamic magnetic field pole near the static magnetic field pole is stronger and the value under the dynamic magnetic field pole far from the static magnetic field pole is about half. Initially, the experiment was conducted on the assumption that Type A, which can set the optimum bias magnetic field, is superior to Type B. The diameter of the conductor to be wound around the magnetic poles for the dynamic magnetic field shown in Figures 6(a) and 6(b) is 0.56 mm. The number of windings was considered between 5 and 30, with 25 windings having the highest received signal.

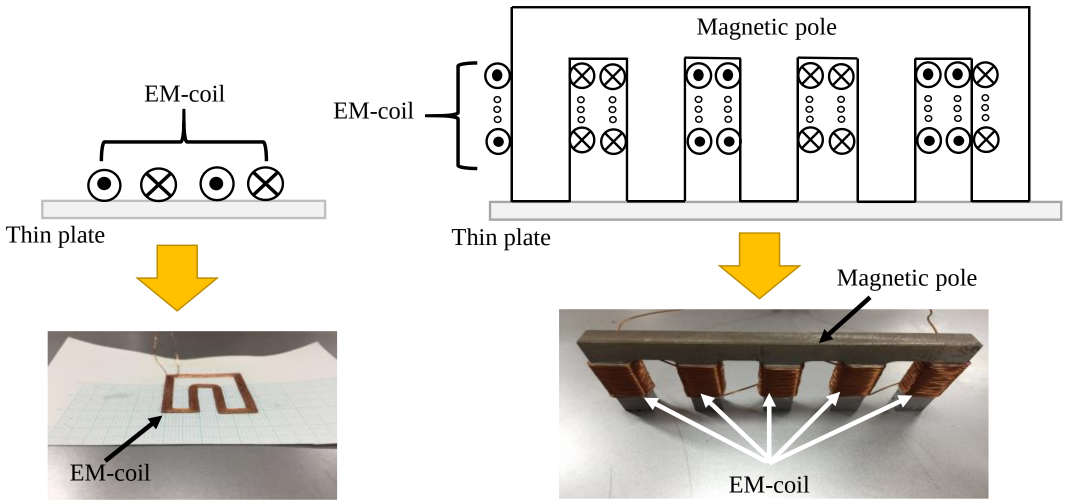

(a)EM-coil for Lamb wave (b)EM-coil with a magnetic pole of a trial EMAT

Fig.4: Basic Concept of Electromagnetic Induction Coil with Magnetic Poles

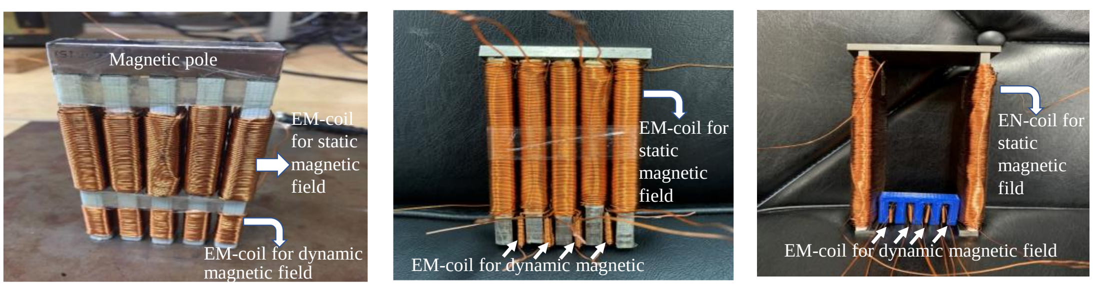

(a) 5 Statics and dynamic magnetic pole are same (b) 5 Statics and dynamic magnetic pole are spatially separated (c) 2 Statics and dynamic magnetic pole are spatially separated

Fig.5: Photograph of the EMAT for Lamb waves using electromagnetic induction coils with magnetic poles

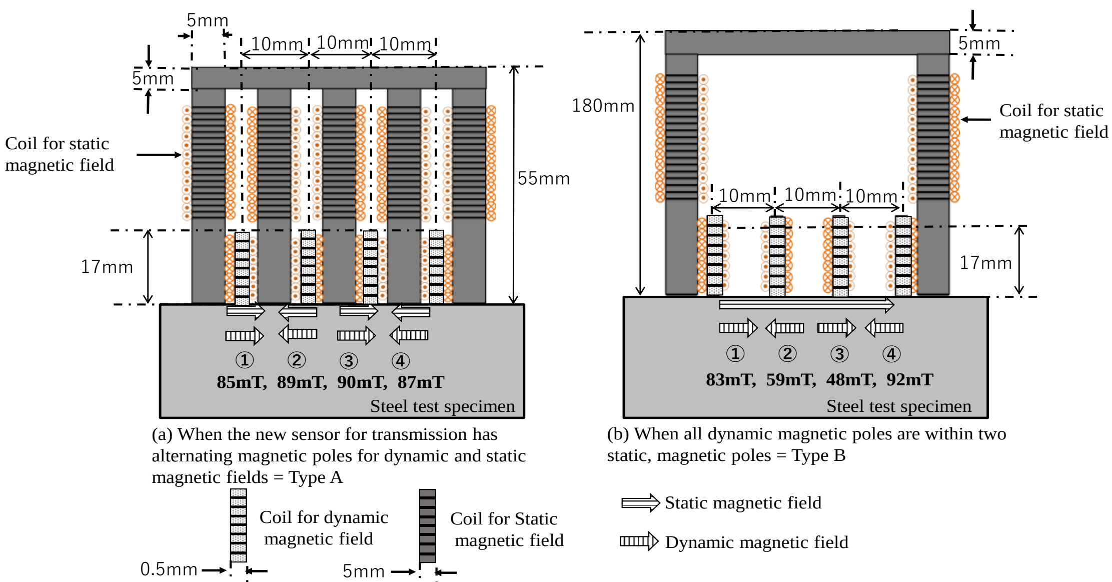

(a) When the new sensor for transmission has alternating magnetic poles for dynamic and static magnetic fields = Type A

(b) When all dynamic magnetic poles are within two static, magnetic poles = Type B

Fig.6: Transition of EMAT for Lamb waves using electromagnetic induction coils with magnetic poles

EXPERIMENTAL CONDITIONS

The test specimens were made of low carbon steel, with dimensions of 0.8 mm plate thickness, 1000 mm plate width, and 1000 mm plate length. Figure 7 shows the experimental layout. The basic arrangement was that the transmitting EMAT and the receiving EMAT were separated by 500 mm. The driving frequency of 200 kHz, in which the ultrasonic velocity is significantly different from the other modes, so that the zeroth-order mode (S0-mode) of the Lamb wave occurs alone, was used as the driving condition. As a result, the distance between the poles for the dynamic magnetic field was set to 5 mm. In other words, transmission and reception of the Lamb waves with the ultrasonic velocity of approximately 5000 m/s were assumed. To evaluate the performance of the transmitter EMAT and receiver EMAT, as shown in Figure 7(a), only the Type A or Type B shown in Figure 6 was used for the transmitter EMAT, while the conventional type EMAT was used for the receiver EMAT. Next, as shown in Figure 7(b), only the Type A or Type B shown in Figure 6 was used for the receiving EMAT, while the conventional type EMAT was used for the transmitting EMAT. Finally, the transmitted received signal strength was checked using prototype EMATs of Type A or Type B shown in Figure 6 for both the transmitting and receiving EMATs in the arrangement shown in Figure 7(c). Figure 8 shows the electronic circuit for driving this EMAT. 200 kHz burst-type sine wave (for four cycles) generated by the waveform generator was amplified to ±75 V by a power amplifier and energized in the coils for the dynamic magnetic field that make up the transmitting EMAT. A direct current was also applied to the coil for the static magnetic field from a DC power supply. The voltage value of the DC power supply was adjusted to maximize the received signal strength. The receiving EMAT was also connected to a preamplifier and a discriminator to the coils for the dynamic magnetic poles, and the amplification factor was set to 100,000 times and the frequency filter from 50 kHz to 500 kHz. In both arrangements, the distance between the transmitting and receiving EMATs was 500 mm. In other words, the sound velocity of the S0 mode lamb wave is about 5400 m/s at a driving frequency of 200kHz, so the propagation time is about 93μs.

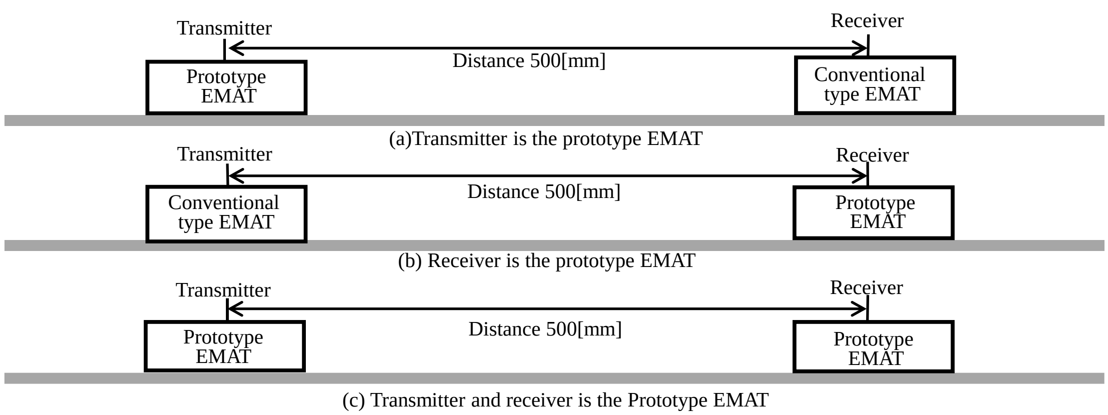

Fig.7: Experimental layout

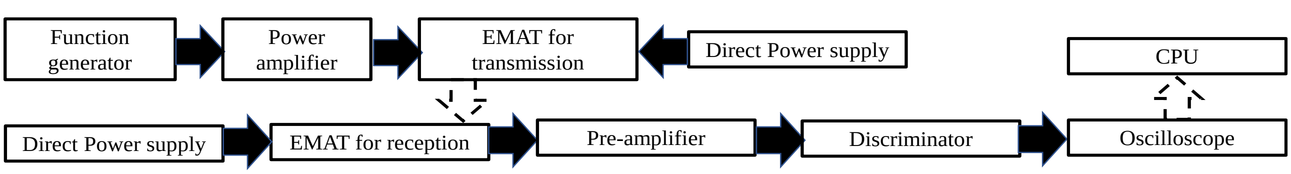

Fig.8: Electric equipment block

EXPERIMENTAL RESULTS

When Only the Transmitting EMAT is Type A or Type B

Figure 9 (a) shows the case where the transmitting EMAT is Type A. The transmitted received signal strength detected at a propagation time of about 90μs was 2.7Vpp. Figure 9(b) shows the case when the transmitting EMAT is Type B. The transmitted received signal strength detected at a propagation time of about 90μs was 18.5Vpp.

When Only the Receiving EMAT is Type A or Type B

Figure 9 (c) shows the case where the receiving EMAT is type A. The transmitted received signal strength detected at a propagation time of about 90μs was 0.9Vpp. Figure 9(d) shows the case when the EMAT for reception is Type B. The transmitted received signal strength detected at a propagation time of about 90μs was 10.8 Vpp.

Cases in Which Both the Transmitting and Receiving EMATs are Type A or Type B

Figure 10(a) shows the case when the transmitter/receiver EMAT is Type A. The transmitted received signal strength was detected at about 90μs, but it is difficult to evaluate the signal strength on this vertical axis scale. Figure 10(b) shows the same case with the Type A EMATs for the transmitter and receiver, but the vertical axis scale is expanded to 0.016Vpp. Figure 10(c) shows the transmitted received signal strength of 3.0Vpp detected at 90 μs when the transmitter and receiver EMATs are Type B.

Comparison of Type A and Type B EMATs

Figure 11 summarizes the evaluation results. In the case of the EMAT for transmission, type B resulted in a 7.2 times greater received signal strength than that for type A. In the case of the receiving EMAT, the received signal strength of type B was 14.6 times more sensitive than that of type A. In the case of the prototype EMATs for both transmitting and receiving, type B resulted in a 101 times greater received signal strength than type A.

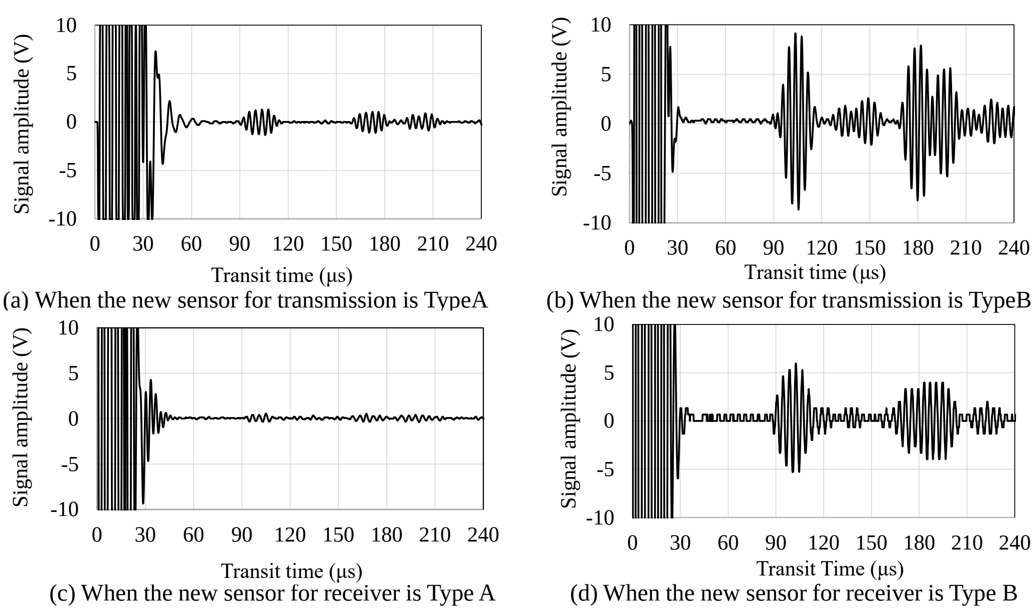

Fig.9: Received signal waveform-When only the transmitting or receiving sensor is a conventional type EMAT

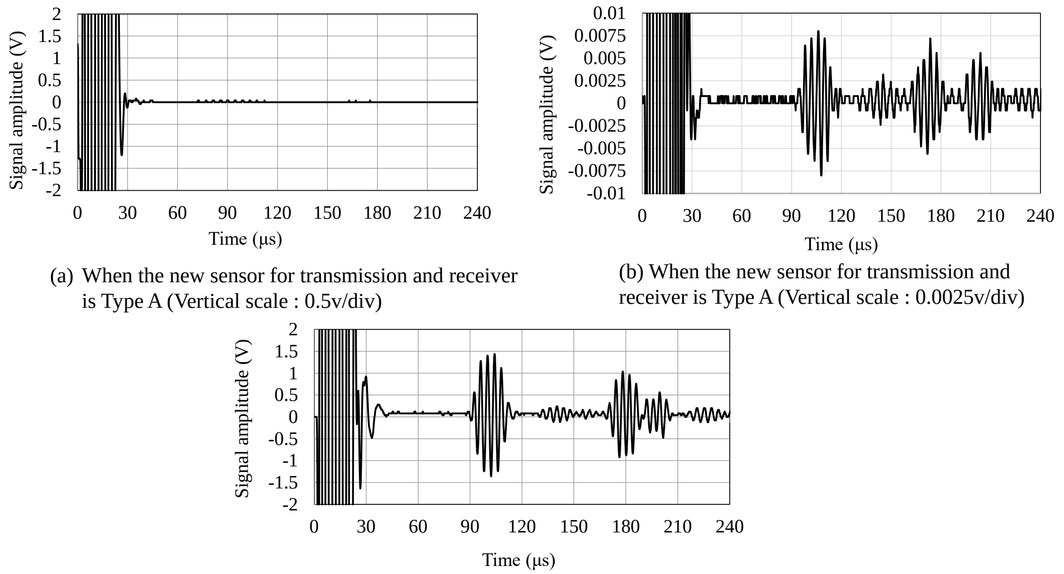

(a) When the new sensor for transmission and receiver is Type A (Vertical scale : 0.5v/div)

(b) When the new sensor for transmission and receiver is Type A (Vertical scale : 0.0025v/div)

(c) When the new sensor for transmission and receiver is Type B

Fig.10: Received signal waveform-When transmission and receiver sensor is a Type A or Type B

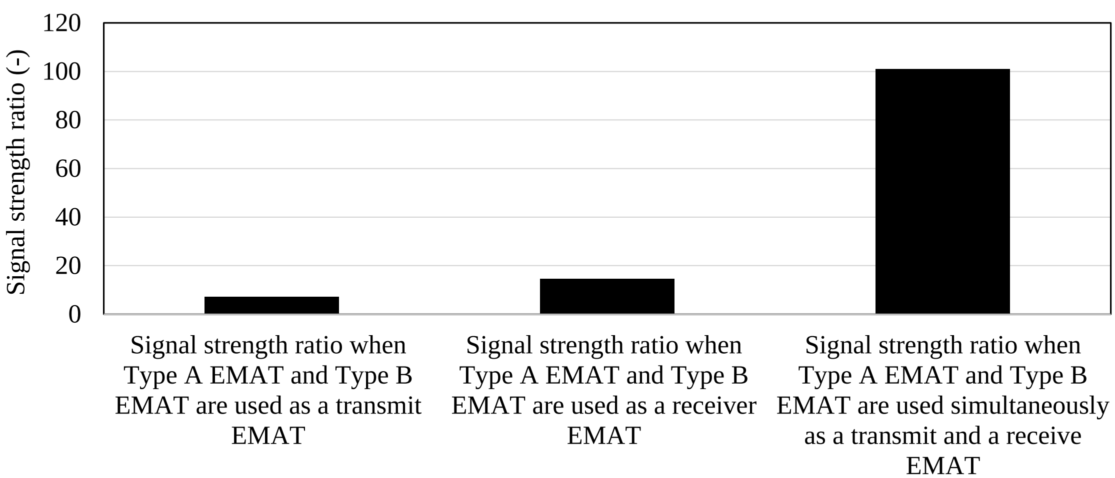

Fig.11: Received signal strength ratio by type A EMAT and type B EMAT

DISCUSSION

The basic idea of Lamb wave EMAT using the magnetostriction effect is to add a bias magnetic field to a ferromagnetic material in which the magnetostriction is most likely to change in response to changes in the magnetic field. As shown in Figure 12, ferromagnetic materials have conditions where magnetostriction fluctuations do not occur easily for the magnetic field fluctuations, as shown in locations ① and ②. On the other hand, in locations ③ and ④, large magnetostriction changes occur for the same magnetic field variation. At first, we focused on providing the bias magnetic field directly below the dynamic magnetic field pole, where the largest magnetostriction variation occurs, without considering the directionality of the magnetostriction. Therefore, we gave priority to Type A, i.e., five-pole EMATs, because the bias field strength can be easily adjusted for each dynamic field pole.

However, once again, consider the case where a bias magnetic field is given in the right direction and the case where a bias magnetic field is given in the left direction, using Figure 13 for the case where a dynamic magnetic field is given in the same direction. At the location ① in Figure 12, if a dynamic magnetic field in the right direction is given, the magnetostriction will increase. However, at the location ② in Figure 12, the magnetostriction decreases when a dynamic magnetic field in the right direction is given. In other words, the magnitude of the magnetostriction fluctuation is the same, but the phase of the increase or decrease is 180 degrees different.

This phenomenon is examined once again in Figure 14, which simulates type A and type B EMATs. Originally, the magnetostrictive fluctuations directly under the poles of the dynamic magnetic field are assumed to be in the opposite direction, but in the case of Type A, the direction of the magnetic field fluctuations is the same even if the dynamic magnetic field is opposite. On the other hand, in the case of Type B, the magnetostrictive fluctuations directly under the adjacent dynamic magnetic field are in the opposite direction, as assumed.

Type A was originally developed based on the advantage that the bias magnetic field directly under all dynamic magnetic field poles can be easily adjusted to the optimum value. The bias fields directly under each dynamic magnetic pole of the EMAT of Type A have a mean value of 87.8 (mT) with a standard deviation of 2.2 (mT), which is considered to be a sufficiently small deviation. On the other hand, the EMAT for the Type B has a mean value of 70.5 (mT) with a standard deviation of 20.5 (mT), which is not considered to be an ideal bias magnetic field distribution. Nevertheless, it is concluded that the bias magnetic field could not compensate for the effect of its direction reversal directly below the adjacent dynamic magnetic field pole.

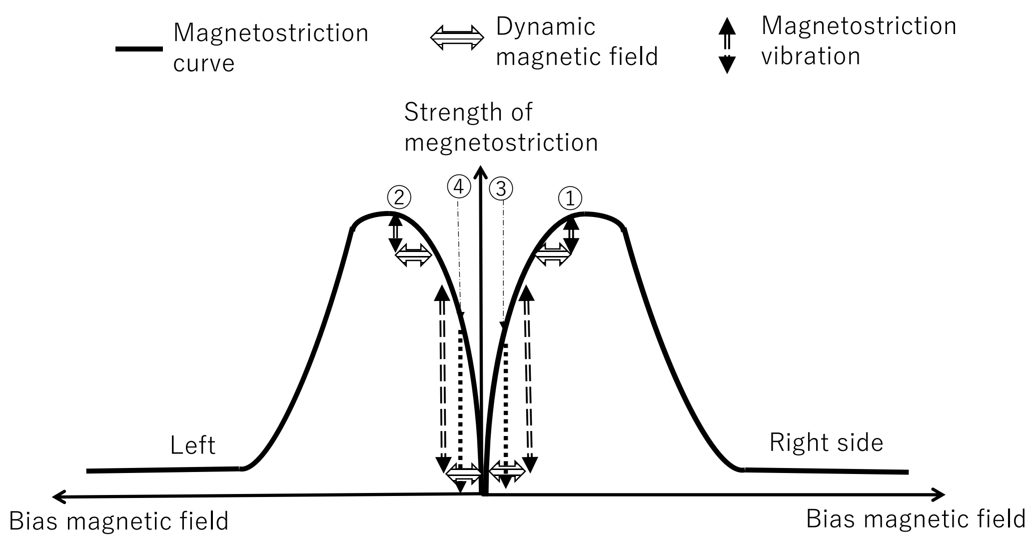

Fig.12: Assumptions at the start of development

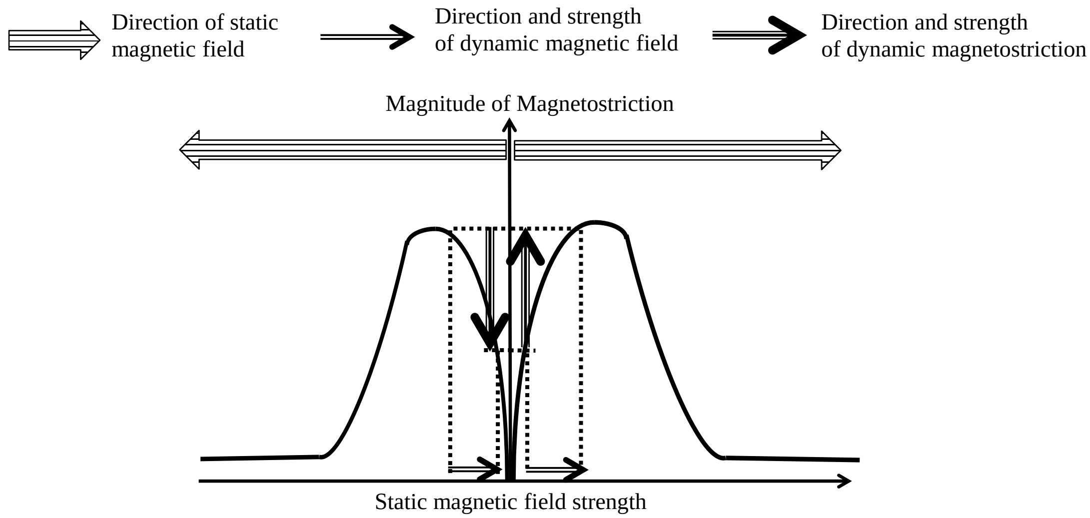

Fig.13: Direction of change of magnetostriction due to induced magnetic field under adjacent dynamic magnetic poles of both types of EMATs

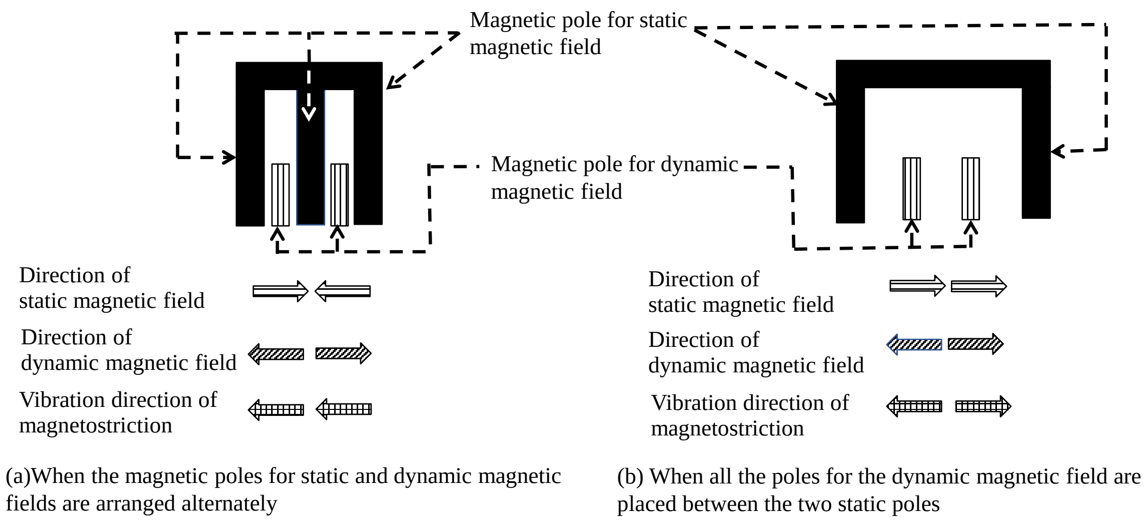

Fig.14: Difference in vibration patterns of two types of EMATs for Lamb waves just below the magnetic poles for dynamic magnetic fields

SUMMARY

Aiming to improve the heat resistance and mechanical shock resistance, which are issues for general Lamb wave EMATs, we have attempted to adopt a ferromagnetic pole insertion type electromagnetic induction coil instead of an air-core type electromagnetic induction coil with a comb shape. So far, we have studied a structure in which the magnetic poles for dynamic and static fields are alternately arranged to optimize the magnetic field strength directly under the dynamic magnetic pole and to provide a bias field of the same strength directly under any of the dynamic magnetic poles.

However, in the present study, a dramatic improvement in the received signal strength was achieved by employing two static magnetic field poles in a configuration that sandwiches all the dynamic magnetic field poles. In this case, it was confirmed that it is extremely important to provide a bias magnetic field in the same direction directly under any dynamic magnetic field pole, although the magnetic field strength directly under each dynamic magnetic field pole is not an optimal value.

References

[1] Peter C, A. and David A., The use of Lamb waves for the long range inspection of large structures, Ultrasonics, 1996.34: p.287-290.

[2] Cawley P., The rapid non-destructive inspection of large composite structures, Composites, 1994.25: p.351-357.

[3] Alleyne D. N., Pavlakovic B. M. J., Lowe M.J.S. and Cawley P., Rapid long-range inspection of chemical plant pipework using guided waves Insight, 1994.43: p.93-96

[4] Saito T. and Fujimori N., Shimizutechnonews, 1980.32: p.69-72 (in Japanese)

[5] Lowe M.J.S., Alleyne D.N. and Cawley P., Defect detection in pipes using guided waves, Ultrasonics, 1998.36: p.147–154.

[6] Lee H., Park H.W. and Sohn H., Pipe defect visualization and quantification using longitudinal ultrasonic modes, Int. J. Structural Stability Dynamics, 2014.14(5): 1440008.

[7] Li. J. and Rose J.L., Natural beam focusing of non-axisymmetric guided waves in large-diameter pipes, Ultrasonics, 2006.44(1): p.35–45.

[8] Leonard K.R. and Hinders M.K., Guided wave helical ultrasonic tomography of pipes, Journal of Acoustic Society of America, 2003.114(2): p.767–774.

[9] Thompson R.B., Experiments in the use of guided ultrasonic waves to scan structures, Review of Progress in Quantitive NDE, 1997.16(A): p.21-128.

[10] Hirao M. and Ogi H., EMATs for science and Industry-Noncontacing Ultrasonic Measurements, Kluwer Academic Publishers 2003: p.1-102.

[11] Sungho C., Hwanjeong C., Matthew C.S. and Cliff J.L., Electromagnetic acoustic transducers for robotic nondestructive inspection in harsh environments, Sensors, 2018.18: https://doi.org/10.3390/s18010193

[12] Dobmann G., Development and Application of EMAT in Warm and Hot Conditions, Journal of The Japanese Society for Non-Destructive Inspection 2004.63: p.1-12.

[13] Murayama R., Qiang L. and Watanabe T., Development of an electromagnetic acoustic transducer using a complex magnetic pole for direct and alternating current, Transactions of the JSME (in Japanese), 2019.85: p.1-12.

[14] Murayama R. and Akizuki Y., Sensors and Actuators A Physical, 2022.333: 113294.